

Static and dynamic properties of localized Mn moments in liquid bismuth

R. Dupree,* R. E. Walstedt, and F. J. DiSalvo

Bell Laboratories, Murray Hill, New Jersey 07974

(Received 6 November 1978)

We present measurements of static susceptibility and of ^{55}Mn and ^{209}Bi NMR shifts and relaxation times over temperatures ranging from 700 – 1400 K for a series of dilute alloys of Mn in liquid Bi. The Mn impurities, which possess a local moment similar to that of CuMn , are found to exhibit a Kondo temperature $T_K \sim 50$ K. A plot of ^{55}Mn shift versus measured impurity susceptibility reveals a small temperature-independent susceptibility term in addition to the Curie-Weiss term. The fluctuation rate of the Mn moment is deduced from relaxation measurements of the ^{55}Mn nuclei, yielding a single-ion term in good agreement with the dynamic susceptibility model for Kondo systems given by Götze and Schlottmann, and a spin-spin Ruderman-Kittel-Kasuya-Yosida (RKKY) term in reasonable accord with realistic model calculations for near-field RKKY exchange. Failure of the ^{209}Bi shift to follow the Mn susceptibility is attributed to temperature-dependent transferred hyperfine coupling; a successful interpretation of this effect is made using x-ray and neutron-diffraction results to determine the temperature-dependent radial distribution function and employing a simple asymptotic model of the RKKY spin-density oscillations. The RKKY amplitude so determined is found to be anomalously large, while the phase (at near-neighbor distances) is in agreement with a recent model calculation for CuMn . By applying a small correction to the moment fluctuation times from liquid motion, we are also able to obtain a quantitative interpretation of the ^{209}Bi relaxation times.

I. INTRODUCTION

Nuclear magnetic resonance has proved to be a key technique in the study of both static and dynamic properties of Kondo impurity systems.¹⁻³ Such studies have provided the major source of confirmation for available theoretical results.⁴⁻⁶ In the present paper we present an NMR study of a rather unusual Kondo system, namely Mn impurities in liquid Bi ($T_K \sim 50$ K). In addition to its being, to our knowledge, the first detailed study of Kondo phenomena in a liquid-metal host,⁷ this system offers several other advantageous features as well. The low melting point of Bi metal ($T_M < 700$ K) allows convenient study over a relatively wide range of temperature. The liquid state eliminates extraneous static NMR line broadening effects; thus one may analyze relaxation phenomena without the attendant ambiguities of quadrupolar broadening. Most interestingly, we may for the first time study the dynamics of the Kondo moment directly through the responses of its own (^{55}Mn) nucleus.⁸ The ^{55}Mn hyperfine coupling is modulated by $s-d$ exchange scattering of conduction electrons and also by indirect (RKKY⁹) exchange at a rate which scales with concentration. By studying the ^{55}Mn relaxation as a function of both temperature and concentration,

these effects can be analyzed separately. The $s-d$ scattering rate is compared with models of Kondo dynamics.⁶

We have also carried out a study of the ^{209}Bi NMR shift and relaxation time in these alloys. One finds the rather surprising result that the ^{209}Bi shift ΔK_{Bi} relative to that of Bi metal does not follow the Mn impurity susceptibility, suggesting a temperature-independent transferred hyperfine coupling. Moreover, there is a strong Mn-induced relaxation mechanism for the ^{209}Bi which also behaves somewhat differently with temperature from the ^{55}Mn relaxation. We analyze these effects using the x-ray and neutron scattering data for the temperature variation of the radial distribution function in a simple asymptotic model for the transferred (RKKY) hyperfine coupling and the local-moment fluctuation times extracted from the ^{55}Mn relaxation measurements. The shift data serve to determine the RKKY phase and amplitude. By introducing a liquid-motion correlation rate estimated from kinetic theory, which acts in parallel with the local-moment spin-lattice relaxation time T_{1e} , we then give a quantitative account of the ^{209}Bi relaxation data.

In Sec. II we discuss sample preparation and experimental technique. The experimental results are presented and analyzed in Sec. III. Our conclusions are summarized in Sec. IV.

II. SAMPLE PREPARATION AND EXPERIMENTAL TECHNIQUE

Certain difficulties were encountered in trying to make reproducible specimens of *BiMn*. For this reason several sample preparation techniques were used. At the outset weighed quantities of 99.999%-purity powdered Bi and 99.9%-purity powdered Mn were mixed with an approximately equal volume of 3.0-micron Al_2O_3 powder and sealed off inside a quartz tube of suitable size for the NMR spectrometer. Before sealing, the material was heated to several hundred °C to drive off adsorbed water. Sealed specimens were then left overnight at 1100 °C, causing the Mn to diffuse uniformly throughout the Bi particles by vapor transport. The Al_2O_3 served to prevent the liquid Bi droplets from coalescing, so that rf fields would penetrate the resulting alloy. The problem encountered with this method was that roughly the first 10 at. % of Mn would simply be lost, presumably to oxidation. Such a loss caused severe difficulties in determining the actual resulting alloy concentration and also led to concentration inhomogeneities.

Substantial improvement was achieved by using, instead of commercial powdered Bi metal, Bi powder filed from the bulk in an inert (argon) atmosphere. With this method far less of the Mn fraction was lost, suggesting adsorbed O_2 or BiO coating in the commercial Bi powder to be the cause of our earlier problems. Even so, we were not certain that we could rely on the nominal concentrations, nor can one be fully confident of chemical analysis on such specimens.

The third and most successful approach was that of using bulk samples fused from etched pieces of Bi and Mn metals (in dilute HCl and HNO_3 , respectively). These were again sealed off under vacuum, before being melted together in an rf induction furnace. There was a much reduced loss of Mn with this method. An ingot with a nominal atomic fraction of 11.75% Mn was divided into five pieces for chemical analysis. The analyzed concentrations averaged $11.0 \pm 0.3\%$, showing a Mn loss equal to 0.75% of the bismuth content. There is evidence in the shift measurements (Sec. III) of similar losses in lower concentration specimens.

The bulk samples were found to have adequate sensitivity for the ^{209}Bi NMR studies. The powdered samples described above were used for most of the ^{55}Mn work in spite of the difficulties in determining concentrations because of the greater sensitivity required. Spot checks were made with bulk samples to corroborate the results.

The NMR relaxation times and most of the shift measurements were made using a conventional pulsed NMR spectrometer operating in the 10–17 MHz range, although some of the shift data were taken with a Varian wide line spectrometer. Signal

quality was improved by accumulating repetitive field sweeps in a Nicolet Model 1072 instrument computer. Sample temperatures were stable to 1 °C and were measured using a Pt–Pt + 10-at. %–Rh thermocouple to an absolute accuracy of 10 °C. Temperature gradients across the sample were also of this order. Susceptibility measurements were made with a conventional electrobalance using bulk alloy specimens.

III. EXPERIMENTAL RESULTS AND DISCUSSION

A. Mn impurity susceptibility

Susceptibility measurements were performed on bulk samples having analyzed concentrations of 2- and 5-at. % Mn, at temperatures ranging from 700 to 1300 K. These measurements were corrected for the background susceptibility contributions of the Bi matrix and the sample holder and then least-squares fitted to a Curie-Weiss law.¹⁰ Fitting parameters p_{eff} and Θ are given in Table I, where the susceptibility is expressed as

$$\chi_{\text{Mn}} = N_m p_{\text{eff}}^2 \mu_B^2 / 3k_B(T + \Theta),$$

N_m being the number of moles of Mn in the sample.

Our results show a significant reduction of p_{eff} from the free spin value ($p_{\text{eff}} = 5.92$) for $S = \frac{5}{2}$ and also a slight apparent dependence of p_{eff} on concentration, both in accord with previous work.¹¹ In addition, our somewhat greater resolution reveals a well-defined Curie-Weiss Θ for this system which was not reported earlier. We interpret Θ to be a Kondo condensation temperature T_K for the Mn moment. It is interesting to contrast this behavior with that of *CuMn*, which has a similar value for p_{eff} ,¹² but has a Kondo temperature that is orders of magnitude lower.¹³

B. ^{55}Mn shift and relaxation

The ^{55}Mn NMR shift has been measured over the range of temperatures from 700 to 1300 K in powdered samples of concentration 1.8, 3, and 6.7

TABLE I. Values of $p_{\text{eff}} = g[S(S+1)]^{1/2}$ and the Curie-Weiss temperature Θ for Mn impurity susceptibilities [$\chi \propto (T + \theta)^{-1}$] in liquid Bi at the Mn concentrations shown.

<i>c</i>	p_{eff}	θ (K)
0.02	5.02 ± 0.1	40 ± 10
0.05	5.17 ± 0.1	60 ± 15

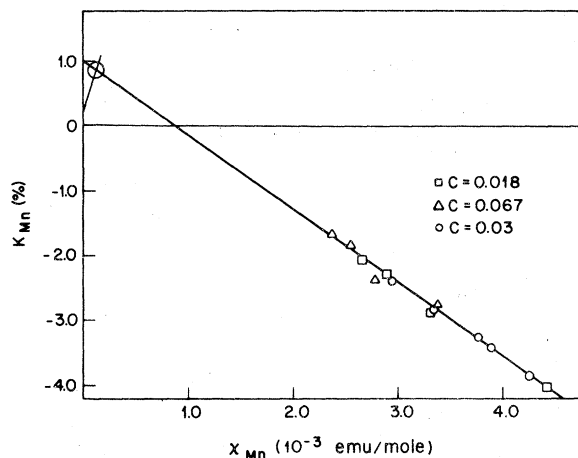


FIG. 1. Plot of ^{55}Mn shift vs Mn impurity susceptibility for three concentrations of $\text{Bi}_{1-x}\text{Mn}_x$ as described in text. Circled intersection of lines shows analysis into spin and orbital components (see text).

at. %. The results are plotted against measured χ_{Mn} values in Fig. 1, where the $c = 2$ at. % χ data are used for the 1.8- and 3-at. % shift results and the $c = 5$ at. % χ data for the 6.7-at. % results. The three sets of data points are seen to follow a well-defined straight line, which is perceptibly improved by selective use of χ data stated above. Following the usual interpretation of $K-\chi$ plots¹⁴ the straight-line behavior is attributed to a ^{55}Mn shift contribution proportional to the temperature-dependent d -spin susceptibility. The slope is then $\alpha_d = H_{\text{hf}}^d / N_0 \mu_B$, where H_{hf}^d is the d -spin hyperfine field per Bohr magneton and N_0 is Avogadro's number. From the plot we find $\alpha_d = -11.3 \pm 0.6$ (emu/mole)⁻¹ (or $H_{\text{hf}}^d = -63 \pm 3$ kG/ μ_B), which is very close to the value found for CuMn .⁸

The positive intercept of the $K-\chi$ curve on the shift axis in Fig. 1 indicates the presence of another, temperature-independent shift contribution.¹⁵ This shift is larger than any possible s -contact shift,¹⁶ and we tentatively attribute it to orbital sources. To continue the analysis we estimate an s -contact shift of 0.2%, and construct a line from the point $K_{\text{Mn}} = 0.2\%$, $\chi_{\text{Mn}} = 0$, with a slope equal to the orbital shift coefficient

$$\beta = K_{\text{orb}} / \chi_{\text{orb}} \sim 65 \text{ (emu/mole)}^{-1},$$

which is estimated from atomic calculations.^{14,17} The intersection of this line with the line through the data points then gives $K_{\text{orb}} \sim 0.65\%$, $\chi_{\text{orb}} \sim 10^{-4}$ emu. It is important to note that such a shift is absent in CuMn , but does appear in $\text{Cu}_{1-x}\text{Al}_x\text{Mn}$ for small x ,⁸ even though the local-moment parameters vary only slightly with x for $0 \leq x \leq 0.2$.¹⁸ We therefore associate such a shift with increased volume density

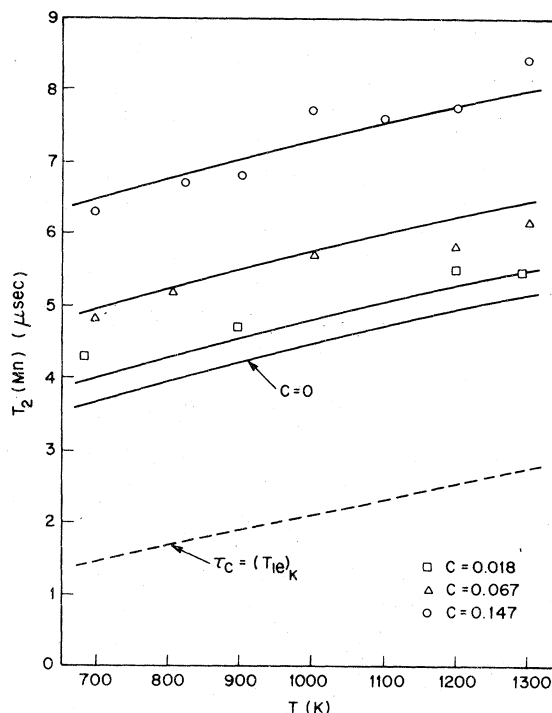


FIG. 2. Measured transverse relaxation times of ^{55}Mn for several concentrations of Mn in Bi, plotted vs temperature. The solid lines are from the model fit described in text and the dashed line corresponds to a Korringa-like variation of the Mn moment fluctuation rate.

of conduction electrons as is indeed found in BiMn . Its appearance could signal the onset of another ionic configuration at the Mn site in the type of picture expounded by Hirst.¹⁹

The ^{55}Mn spin-lattice relaxation time was studied through measurements of the free-induction decay time T_2 , which was presumed equal to T_1 in the liquid state.²⁰ Data for T_2 vs T for three concentrations²¹ of ^{55}Mn are shown in Fig. 2. T_2 is extremely short in comparison with expected contributions from the conduction band. We therefore conclude that this process is dominated by the local-moment fluctuation mechanism identified in CuMn .⁸ The two most striking features of these data are, first, that T_2 becomes longer as the concentration is increased, and second, that the temperature variation is weaker than the linear T law based on "normal" Korringa relaxation of the local moment.

We analyze the T_2 data using the Kondo effect model theory developed by Götzke and Schlottmann⁶ (GS) in which the local-moment $s-d$ exchange fluctuation rate T_1^{-1} is found to vary approximately as $T^{(1-2\rho/J)}$ at high temperatures,²² where J is the $s-d$ exchange coupling and ρ is the host band density of states for one spin direction at the Fermi surface. The concentration dependence is ascribed to RKKY

TABLE II. Local-moment fluctuation lifetime parameters obtained by least-squares fitting Eqs. (1) and (2) to the data of Fig. 2.

A (sec K ⁻¹) ⁻⁵	α	τ_{RKKY} (sec)
$(1.0 \pm 0.5) \times 10^{10a}$	0.55 ± 0.07	$(1.33 \pm 0.09) \times 10^{-13}$

^aParameter A is highly correlated with α in the fitting procedure. For fixed α , A is determined to $\sim 5\%$.

exchange coupling between the Mn impurity moments. The combined nuclear relaxation effect of T_{1e} and the RKKY exchange fluctuations can be described by

$$1/T_1 = \left(\frac{2}{3}\right) (\alpha_d \gamma \mu_B p_{\text{eff}} N_0)^2 \tau_c, \quad (1)$$

where τ_c is the correlation time of the local-moment hyperfine fluctuations. The observed behavior of T_1 corresponds to a shortening of τ_c with increasing concentration. The combined effects of T_{1e} and RKKY fluctuations can be approximated as follows. The autocorrelation decay rate τ_c^{-1} is presumed to be increased, on the average, by an amount proportional to the mean number zc of Mn neighbors to a given Mn site. Thus,

$$1/\tau_c = 1/T_{1e} + cz/\tau_{\text{RKKY}}, \quad (2)$$

where τ_{RKKY}^{-1} is the exchange fluctuation rate per Mn neighbor and z is the coordination number of the liquid. For $c \rightarrow 0$ Eq. (1) then reduces to the well-known results for isolated impurities.²³ One would expect τ_{RKKY} to vary only slowly with temperature. Thus, from Eqs. (1) and (2), one expects plots of T_1 (T_2) vs T for various concentrations to consist of similar curves displaced vertically by amounts proportional to c , as is indeed found (Fig. 2).

From the above analysis we are able to derive a quantitative measure of T_{1e} vs T , since all the other parameters in Eq. (1) are known. To this end we have carried out a least-squares fit of Eqs. (1) and (2) to the data, adopting the form $T_{1e}^{-1} = AT^\alpha$, where $\alpha = 1 - 2\rho|J|$ for the $S = \frac{1}{2}$ case analyzed by GS. The fitting parameters are therefore A , α , and τ_{RKKY} , where we take $\alpha_d = -11.3$ (emu/mole)⁻¹ from above and $z = 8.8$ from radial distribution measurements.²⁴ The resulting curves for T_2 are shown in Fig. 2 as solid lines, with parameter values collected in Table II. A satisfactory fit is achieved in this way, with the main errors arising from uncertainties in experimental concentrations.

In Fig. 2 the variation of T_{1e}^{-1} with temperature is shown in the curve labeled " $c=0$." To compare these

results with the GS model theory we estimate the Korringa rates assuming $l=2$ symmetry for the $s-d$ exchange coupling. Assuming the mixing exchange is dominant, then $p_{\text{eff}} = (1 - 5\rho|J_2|/2)p_{\text{eff}}$ (free spin).²⁵ The experimental value (5.1) then yields $\rho|J_2| = 0.055$, which may be an overestimate in view of corresponding results for Cu Mn.²⁵ The local-moment Korringa rate is then

$$(T_{1e})_K^{-1} = 5\pi(\rho J_2)^2 k_B T / \hbar, \quad (3)$$

and is plotted as a dashed line in Fig. 2. Thus T_{1e}^{-1} is seen to exceed the Korringa rate by a considerable factor, as predicted by GS. We also make a quantitative comparison with the GS results for T_{1e}^{-1} , which were calculated assuming $\rho J = 0.2$ or $1 - 2\rho J = 0.6$. This is reasonably close to our fitted value $\alpha = 0.55$. Using the $T^{(1-2\rho|J|)}$ law to extrapolate the values from GS (Fig. 8, Ref. 8) to $T = 700$ K ($T/\Theta = 17.5$) and $T = 1300$ K ($T/\Theta = 32.5$), the GS model calculation predicts a Korringa enhancement $[(T_{1e})_K/T_{1e}]$ of 3.1 ± 0.3 and 2.4 ± 0.3 , respectively. The corresponding experimental ratios (Fig. 2), which are 2.5 and 1.9, respectively, have a variation with temperature similar to the GS model but are somewhat lower. This may be because our estimate of ρJ_2 (based on p_{eff}) leads to an underestimate of $(T_{1e})_K$.²³ We also note that our slightly larger value for ρJ (than that used by GS) would lead to improved agreement with experiment.

The fitted value of α (Table I) for the power law dependence of T_{1e}^{-1} has rather broad error limits and lies between the "static" value $2(2l+1)\rho J_2 = 0.62$ and the "dynamic" [i.e., as in Eq. (3)] value $2(2l+1)^{1/2}\rho J_2 = 0.28$. Unfortunately, one cannot say from the $S = \frac{1}{2}$ results just how α is modified in the case of $l=2$ symmetry. We therefore consider the present correspondence satisfactory until such time as $l=2$ model results become available.

Finally, it is interesting to compare the value of τ_{RKKY} with available theories of RKKY exchange as well as other experimental evidence. Caroli²⁶ has extended Yosida's earlier treatment⁹ of RKKY exchange to include $l > 0$ components of $s-d$ exchange coupling. Treating liquid Bi as a free-electron metal with 5 electrons/atom and using the nearest-neighbor distance (3.38 Å) and coordination number (8.8) for liquid Bi given by Waseda and Suzuki,²⁴ we estimate

$$\tau_{\text{RKKY}}^{-1} \sim J_{\text{nn}} S / \hbar \sim 10^{14} \text{ sec}^{-1},$$

which is an order of magnitude faster than the fitted value (Table II). However, Malmstrom *et al.*²⁷ have shown in a realistic model calculation that the near-field RKKY exchange coupling is greatly reduced from its asymptotic amplitude $\propto r_{ij}^{-3}$ at nearest-neighbor distances. Thus the "discrepancy" noted is

not surprising. Further, it is interesting to compare these results with the exchange rate implied by the ordering temperature of ferromagnetic BiMn, $kT_c \sim ZJS$. Using $Z=6$ and $T_c=630$ K we find $JS/\hbar \sim 1.4 \times 10^{13} \text{ sec}^{-1}$, in good accord with the estimate from τ_{RKKY} .

C. ^{209}Bi NMR shift and relaxation effects due to the Mn impurities

The addition of Mn impurity atoms to liquid bismuth has a strong effect on both the shift and spin-lattice relaxation of the ^{209}Bi . Measured values of these parameters for pure Bi metal²⁸ are plotted against temperature in Fig. 3. The shift of ^{209}Bi with Mn concentration is illustrated in Fig. 4, where we plot $\Delta K_{\text{Bi}} = K_{\text{alloy}} - K_{\text{Bi}}$ versus nominal concentration c at $T=700$ K for the bulk samples described in Sec. II. The straight line drawn through the low-concentration points shows that a quantity of Mn equal to $\sim 1\%$ of the Bi content of the sample is lost in the alloying process. This is in accord with the analysis of the 11.75% sample presented in Sec. II. The slope of the line in Fig. 4 gives $\Gamma = c^{-1} K_{\text{Bi}}^{-1} d\Delta K_{\text{Bi}}/dc = 28$, which is a very large effect. We also note that the $c=0.11$ shift falls well below the linear behavior found at low concentration.

The temperature dependence of ΔK_{Bi} for several concentrations is shown in Fig. 5. There we plot ΔK vs χ_{Mn} . One sees immediately that ΔK_{Bi} and χ_{Mn} have distinctly different temperature dependences.

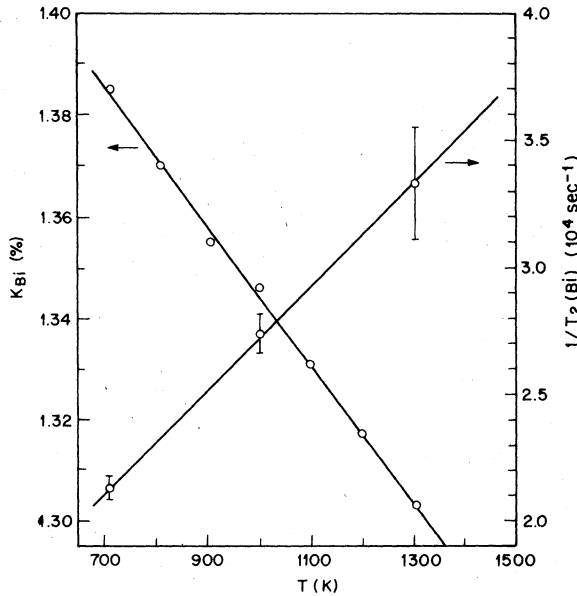


FIG. 3. Frequency shift and (transverse) spin-lattice relaxation of ^{209}Bi in liquid Bi as a function of temperature.

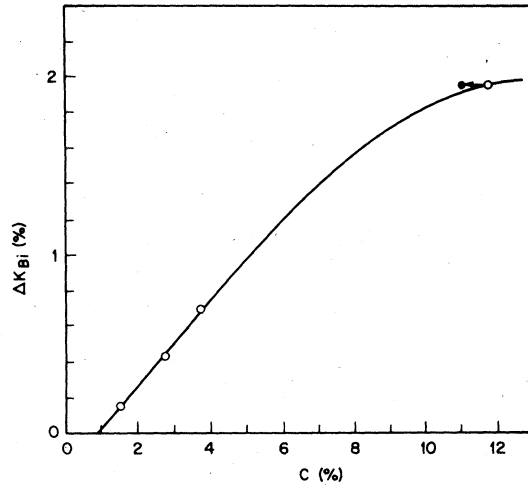


FIG. 4. Measured shift of ^{209}Bi at 1000 K (relative to that of pure Bi) in $\text{Bi}_{1-c}\text{Mn}_c$ as a function of nominal concentration c . The analyzed concentration for $c=0.1175$ is shown as a closed circle.

The behavior of ΔK is very similar to that found for ^{63}Cu in CuMn .²⁹ We find the explanation proposed earlier for this effect²⁹ to be unsatisfactory³⁰; thus we suggest two other possible mechanisms. The first is illustrated by passing a straight line through the data for a single concentration in Fig. 5. The intercept K_0 of this line at $\chi_{\text{Mn}}=0$ ($T=\infty$) might correspond to a change in the (temperature-independent) conduction band shift caused by the added impurities. However, one finds

$$\Gamma_0 = c^{-1} K_{\text{Bi}}^{-1} \frac{dK_0}{dc} = -9$$

for this shift, which is an order of magnitude too large to be realistic. Thus we consider an alternative hypothesis, namely that the failure of ΔK_{Bi} to track χ_{Mn} is the result of a temperature-dependent hyperfine coupling between the Mn spins and the host Bi nuclei. This temperature dependence would stem from that of the radial distribution function as projected against the rapid and (relatively) stationary oscillations of the RKKY hyperfine interaction. We have undertaken a model calculation of this effect, to be presented below, in which the results are successfully accounted for.

Next, we present the data for the measured increase

$$\Delta(T_2^{-1}) = (T_2^{-1})_{\text{alloy}} - (T_2^{-1})_{\text{Bi metal}}$$

in ^{209}Bi spin-lattice relaxation rate due to alloying.³¹ This is plotted as $1/\Delta(T_2^{-1})$ vs T in Fig. 6 for $c=1.8\%$, where we see that there is a very large effect for such a small impurity concentration. The temperature dependence is similar to that of T_2 (Mn)

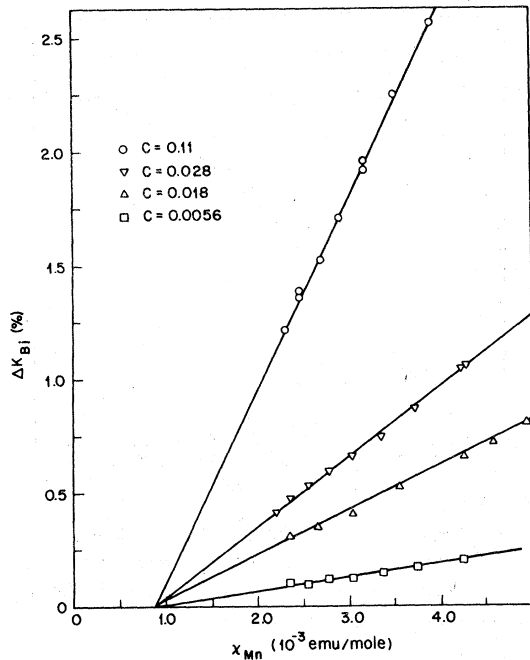


FIG. 5. Measured shifts of ^{209}Bi in several BiMn alloys (relative to that of pure Bi) plotted as a function of manganese impurity susceptibility to illustrate the disparity in temperature dependences. Concentrations shown are analyzed ($c = 0.11$) or deduced from shift behavior.

except that it seems to flatten out at low temperatures. In Ref. 7 a model calculation of $\Delta(T_2^{-1})$ was presented based on fluctuating hyperfine coupling with impurity spins, in which the radial distribution of Bi neighbors to an impurity was treated as a δ function and the transferred hyperfine coupling was estimated from ΔK_{Bi} . This model was found to underestimate $\Delta(T_2^{-1})$ by an order of magnitude, and an additional relaxation mechanism (of unknown origin) was suggested to be present. In the following it is shown that a more realistic treatment of the transferred hyperfine fluctuations leads to a successful understanding of the relaxation data.

We now model the ^{209}Bi shift and relaxation effects caused by magnetic solute atoms in terms of the radial density function $\rho(r)$ for Bi metal³² and an isotropic transferred (RKKY) hyperfine interaction $A_i(r)\bar{I} \cdot \bar{S}$ between a solute spin \bar{S} and a ^{209}Bi nuclear spin \bar{I} separated by distance r . Using the known impurity susceptibility function we then have for the induced shift

$$\Delta K_{\text{Bi}} = \frac{cg_{\text{eff}}\mu_B S(S+1)}{3\gamma k_B(T+\Theta)} \int_0^\infty A_i(r)\rho(r) dr, \quad (4)$$

where g_{eff} is the effective g factor of the local moment in a metallic environment. Equation (4) presumes that the effects of several impurity spins

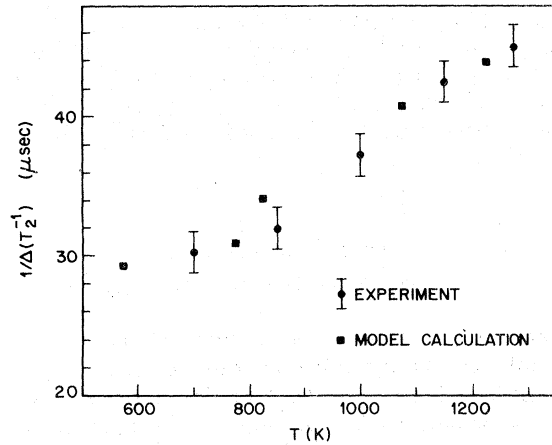


FIG. 6. Inverse of measured increase in ^{209}Bi spin-lattice relaxation rate (relative to pure Bi) for 1.8% Mn in Bi, plotted as a function of temperature. Fitted values from the model calculation described in text are also shown.

superimpose linearly, which will be true at low concentrations. This expression represents an average over all possible environments, and it is presumed that the rapid liquid motion performs this averaging process in a time short compared with T_2 .

The fluctuations in the transferred hyperfine couplings are responsible for $\Delta(T_2^{-1})$; they arise in two ways. First, the spin-lattice relaxation process of the solute spins causes orientational fluctuations at a rate $\sim T_{1c}^{-1}$, and second, the liquid motion causes fluctuations by changing the distance r between a spin \bar{S} and a nucleus \bar{I} . We assign a correlation time τ_l to the latter fluctuations. The precise formulation of the host relaxation depends upon which of the foregoing two mechanisms is predominant. For orientational fluctuations alone we may write

$$\Delta(T_2^{-1}) = \frac{2}{3}cS(S+1)\tau_c \int_0^\infty A_i^2(r)\rho(r) dr, \quad (5)$$

with τ_c given by Eq. (2). Equation (5) is simply a superposition of the effects of impurities at all (fixed) distances using Eq. (1).²³ The liquid-motion hyperfine fluctuations depend, in contrast, on space-time correlation functions of the liquid.³³ We mention these two possibilities because even though $\tau_l > T_{1c}$, the predominance of orientational fluctuations turns out to be marginal in BiMn . In order to avoid undue complexity, however, we shall use Eq. (5) for computational purposes and use a modified correlation time

$$\tau_c = (T_{1c}^{-1} + cz/\tau_{\text{RKKY}} + \tau_l^{-1})^{-1} \quad (6)$$

to account for additional modulation from liquid motion. This should provide a reasonable approximation for the liquid-motion contribution, because contributions to $\Delta(T_2^{-1})$ are strongly peaked at the first-neighbor shell.

Equations (4), (5), and (6) form the basis for our interpretation of the data in Fig. 5 and 6. The procedure is as follows. As a first step we calculate $\rho(r)$ at several temperatures in the range of interest from x-ray and neutron scattering data given by Waseda *et al.*³⁴ This is carried out using

$$\rho(r) = 4\pi r^2 \rho_0 + \left(\frac{2r}{\pi} \right) \int_0^\infty dk k [a(k) - 1] \sin(kr), \quad (7)$$

where ρ_0 , the atomic density of liquid Bi, is given by³⁵

$$\rho_0(T) = 2.897 \times 10^{-2} + 3.64 \times 10^{-6}(T - 544) \text{ atoms/\AA}^3. \quad (8)$$

For the purpose of evaluating Eq. (7) the data for $a(k)$ for $1.2 \leq k \leq 9.0$ are extrapolated smoothly to smaller k values using a power law fitted to the leading edge of the first peak. Extrapolations of the decaying oscillations of $[a(k) - 1]$ to larger k values were also included, but these made only very small corrections in the resulting $\rho(r)$. In spite of these procedures, spurious oscillations were always found in $\rho(r)$ just below the first-neighbor peak.³⁴ These are considered unphysical and are eliminated by extrapolating the leading edge of $\rho(r)$ smoothly to zero. Since the integrals in Eqs. (4) and (5) involve $\rho(r)/r^3$ and $\rho(r)/r^6$, we illustrate the results for $\rho(r)$ by plotting these two quantities for $T = 300^\circ\text{C}$ in Fig. 7. Note that the modulus of the shift integrand [Fig. 7(b)] decays rather slowly as r^{-1} , whereas the relaxation integrand is peaked sharply at the first-neighbor position.

Having obtained $\rho(r)$, we first consider the shift, i.e., Eq. (4). To evaluate the integral we take for convenience⁹

$$A_i(r) = B \cos(2k_F r + \phi) / r^3, \quad (9)$$

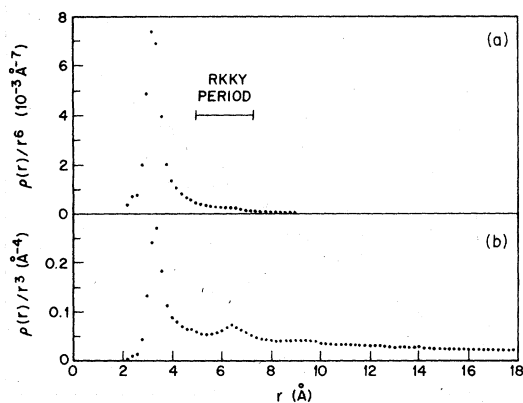


FIG. 7. Envelopes of integrands for induced ^{209}Bi relaxation effect (top) and induced shift (bottom) calculated from neutron and x-ray data for the pair correlation function at 300°C . The tail on the shift envelope decays as r^{-1} .

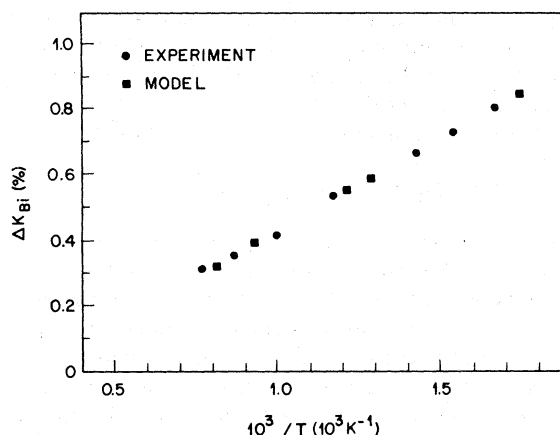


FIG. 8. Induced shift data from Fig. 5 for $c = 1.8\%$ compared with results of model calculation described in text.

where k_F is calculated on a free-electron model assuming 5 electrons/atom. From p_{eff} (Table I) we find $g_{\text{eff}} = 1.73$ assuming $S = \frac{5}{2}$ for the Mn moment. The quantities B and ϕ are then adjusted to best fit $\Delta K_{\text{Bi}}(T)$ for $c = 0.018$, yielding

$$B = (3.6 \pm 0.4) \times 10^{-14} \text{ erg cm}^3$$

and $\phi = 100 \pm 20$ degrees. The resulting fit is shown in Fig. 8 and is seen to be excellent. The temperature dependence of $\rho(r)$ is easily able to account for the shift behavior. Incidentally, the period π/k_F of RKKY oscillations is shown in Fig. 7, where we see that the δ -function approximation employed in Ref. 7 is actually quite poor.

Adopting the values of B and ϕ determined by the shift and T_{1e} from Table II, one then has all parameters except τ_l to complete the calculation of $\Delta(T_2^{-1})$ with Eqs. (5) and (6). To estimate τ_l we argue as follows. Neutron scattering results³⁶ demonstrate that on a time scale of $\sim 10^{-13}$ sec or less the motion of atoms in a liquid is gaslike. Thus, we may take τ_l as the time required for an atom to move a distance over which $A_i(r)$ changes by a significant amount when moving at the mean thermal velocity $\bar{v} = (8kT/\pi M)^{1/2}$ taken from kinetic theory, viz. $\tau_l = d/\bar{v}$. Adjusting d for a best fit to the $c = 0.018$ data in Fig. 6 gives $d = 0.41 \text{ \AA}$. This length corresponds approximately to a phase change of $\frac{1}{2}\pi$ in Eq. (9). One then finds that τ_l varies from 1.5×10^{-13} sec at 700 K to 1.1×10^{-13} sec at 1300 K. Agreement with the data in Fig. 6 is again excellent. In Eq. (6) τ_l^{-1} accounts for $\sim \frac{1}{3}$ of the correlation decay rate. We also note that the temperature dependence of τ_l materially improves the agreement with the data of Fig. 6.

It is interesting to compare the deduced transferred

hyperfine coupling parameters with values from other sources. The magnitude of the transferred coupling is embodied in the constant B , which leads to another estimate of the local-moment-conduction electron exchange interaction according to the formula²⁵

$$B = 5\gamma\Omega K_s J_2^{\text{SDO}} / 8\pi\mu_B, \quad (10)$$

where Ω is the atomic volume, J_2^{SDO} is the exchange parameter appropriate to spin-density oscillations, and K_s is the contact part of the ²⁰⁹Bi shift. To estimate K_s in Eq. (10) one must be careful to note that K_{Bi} is $\sim 25\%$ smaller than one would estimate from T_1 measurements using the Korringa relation with "normal" enhancement³⁷ (estimated from the behavior of similar liquid metals). This discrepancy could result from either an additional strong spin-lattice relaxation mechanism or from a negative core-polarization shift contribution resulting from strong p character at the Fermi surface. Making the conservative assumption that the latter choice is correct, one then finds $|J_2^{\text{SDO}}| \sim 0.38$ eV. Assuming further that $m^*/m \sim 0.87$,³⁸ we find $\rho \sim 0.26$ eV⁻¹ atom⁻¹ and $\rho|J_2^{\text{SDO}}| \sim 0.1$, which is 1.7 times the value estimated from p_{eff} . This is clearly an anomalous result, especially in view of the fact that for CuMn the estimate J_2^{SDO} is actually smaller than that derived from p_{eff} .²⁵ Moreover, if RKKY damping due to smearing of k_F in the liquid state (see below) is significant, the discrepancy could be considerably larger than the estimate above.

One clue to the origin of this anomaly may be that this estimate of J_2^{SDO} comes from the near-field RKKY oscillations as opposed to the asymptotic ($r \rightarrow \infty$) disturbance measured by the inhomogeneous NMR linewidth in the solid.²⁵ Cohen and Slichter³⁹ have recently emphasized that the near-field RKKY oscillations involve contributions from the entire band; thus, ΔK_{Bi} [Eq. (4)] involves a different conduction-band hyperfine interaction which is only poorly estimated by K_s in Eq. (10). In particular, one may speculate that in liquid Bi, with five conduction electrons per atom, the Fermi-surface states may tend to be rather p -like with a correspondingly weak hyperfine interaction, whereas the near-field RKKY effect in Eq. (4) would involve admixture of s character from lower in the band. As a result, Eq. (10) could easily overestimate J_2^{SDO} . It may also be relevant that a Mn impurity atom with ~ 2 band electrons evidently causes a large local disturbance in the conduction band. If these conjectures are true, then $A_i(r)$ would deviate considerably from the form given in Eq. (9), making it somewhat remarkable that a consistent account of ΔK_{Bi} and $\Delta(T_2^{-1})$ is obtained with this equation. On the other hand, the key oscillatory feature of Eq. (9) is probably responsible for its success in the analysis given.

A second experimental parameter to be examined

is the phase ϕ of RKKY oscillations represented by Eq. (9). This may be compared with the results of a recent model calculation of near-field RKKY spin density oscillations which has been applied to CuMn.³⁹ Taking zero crossings in these results to be an indication of RKKY phase, we plot the calculated phase against $2k_F r$ in Fig. 7. At the Bi Mn nearest-neighbor position (see Fig. 9) the calculated phase is seen to lead $2k_F r$ by $\sim \frac{1}{2}\pi$, in good agreement with our deduced value of $\phi \sim 100^\circ$. This agreement may be fortuitous, but it also suggests that the near-field RKKY phase for Mn impurities is not a strongly host-dependent property.

Lastly, we touch upon the question of the smearing of the Fermi surface in k space in the liquid state. Chan and Ballentine³⁸ have considered this effect in a study of conduction-band properties of several liquid metals including bismuth. They report a nearly free-electron-like band having a distribution of Fermi-surface wave vectors of width $\Delta k_F/k_F \sim 0.1$. The effect of this distribution would clearly be to attenuate the time-averaged RKKY oscillation amplitude at any given distance. A crude estimate of the attenuation can be made by simply averaging the RKKY function over the k_F distribution. Assuming a Lorentzian shape³⁸ for the distribution, one finds the RKKY amplitude to be diminished by the factor $e^{-2\Delta k_F r}$. This suggests a reduction of the nn hyperfine coupling by a factor ~ 3 below the value given by Eq. (9), in contrast with the observed enhancement by ~ 1.7 noted above. If the Δk_F estimate of Ref. 34 is realistic, then either the exponential factor overestimates the near-field RKKY damping or the hyperfine ano-

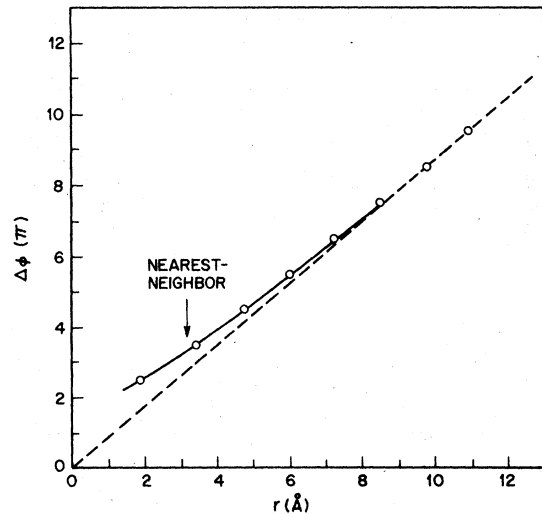


FIG. 9. Deviation of near-field RKKY spin density oscillation phase from its asymptotic value (dashed line) derived from the model calculation of Cohen and Slichter.

mally conjectured above is much larger than was suggested. A good deal of further study will be required to resolve these questions.

IV. SUMMARY AND CONCLUSIONS

In summary, the data presented here identify dilute Mn in liquid Bi as a Kondo system with a Kondo temperature $T_K \sim 50$ K. The Mn moment is very nearly that found in CuMn, leading us to conclude that the $3d^5$, 6S ionic state of Mn^{2+} lies lowest in Bi in spite of the contrasting 5 electron/atom valency of the host metal. However, the $K-\chi$ plot (Fig. 1) reveals a notable deviation from purely S state in behavior, i.e., the presence of a small, temperature-independent contribution to the ionic susceptibility. In the fluctuating electronic environment of the liquid, this may represent occasional circumstances where the Mn moment quenches. It is reminiscent of the behavior of Mn in a copper host with an increasing admixture of aluminum,⁸ where the appearance of a temperature-independent susceptibility term precedes the vanishing of the local moment.

The local-moment fluctuation rates as measured via the spin-lattice relaxation time of the ^{55}Mn nuclei exhibit both single-ion (exchange scattering) and moment-moment (RKKY) contributions, the latter varying in an approximately linear fashion with concentration as expected. Variation of the single-ion fluctuation rate with temperature is found to vary as $T_{1c}^{-1} \propto T^{0.55}$, in reasonable agreement with the model of Kondo dynamics given by Götze and Schlottmann.⁶ We also deduce a value for the RKKY exchange frequency at nearest-neighbor distances, $\tau_{\text{RKKY}} \sim 10^{-13}$ sec, in good accord with a realistic model²⁷ of near-field RKKY coupling.

The ^{209}Bi NMR shift and relaxation rate are both strongly affected by the presence of Mn impurities. The Mn-induced shift of the ^{209}Bi appears to have an anomalous temperature dependence in that it does not follow the Mn susceptibility. Conjecturing that temperature-dependent transferred hyperfine coupling is responsible for this, we have calculated the

effect using a simple asymptotic model for the RKKY spin-density oscillations and employing x-ray and neutron scattering data to estimate the temperature varying radial density function. By optimizing the RKKY phase and amplitude, a quantitative fit to the shift results is obtained. To our knowledge this is the first successful application of radial density function data to temperature-dependent transferred hyperfine effects. A similar anomaly in the temperature dependence of the ^{63}Cu NMR shift in CuMn has been noted.²⁹ We conjecture that the explanation developed here is also applicable in that case.

To calculate the ^{209}Bi relaxation we need only modify the fluctuation rate of the Mn moment slightly to take account of liquid-motion effects. Using all other parameters as determined above, the correlation time for liquid motion that gives quantitative agreement with the ^{209}Bi relaxation data is in excellent accord with an estimate from kinetic theory. Thus, we find that all our results can be accounted for using known physical models and easily estimated parameters. The primary new information gained from the ^{209}Bi results consists of the phase and amplitude of the RKKY spin-density oscillations. The phase is found to agree quite closely with that obtained at near-neighbor distances in a model calculation by Cohen and Slichter³⁹ for CuMn, suggesting that near-field RKKY coupling may be substantially host independent. The RKKY amplitude, however, is considerably larger than what would correspond to a reasonable estimate of $J\rho$. This anomaly is suggested to arise from enhanced participation of deeper-lying s -like states of the Bi conduction band in the near-field RKKY oscillations, as opposed to the more p -like states at the Fermi surface of the pure metal.

ACKNOWLEDGMENTS

The authors wish to acknowledge useful discussions with W. W. Warren, Jr., and the technical assistance of G. F. Brennert.

*Permanent Address: Univ. of Warwick, Coventry, England.

¹J. B. Boyce and C. P. Slichter, Phys. Rev. Lett. **32**, 61 (1974); Phys. Rev. B **13**, 379 (1976).

²H. Alloul, Phys. Rev. Lett. **35**, 460 (1975); J. Phys. (Paris) **37**, L-205 (1976); Physica (Utrecht) **86-88B**, 449 (1977).

³A. Narath, Solid State Commun. **10**, 521 (1972).

⁴P. W. Anderson and G. Yuval, Phys. Rev. Lett. **23**, 89 (1969); P. W. Anderson, G. Yuval, and D. R. Hamann, Phys. Rev. B **1**, 4464 (1970); K. D. Schotte and U.

Schotte, Phys. Rev. B **4**, 2228 (1971).

⁵H. R. Krishna-Murthy, K. G. Wilson, and T. W. Wilkins, Phys. Rev. Lett. **35**, 1101 (1975).

⁶W. Götze and P. Schlottmann, J. Low Temp. Phys. **16**, 87 (1974), also see references therein.

⁷Preliminary report on these results has been given [R. Dupree and R. E. Walstedt, in *Proceedings of the 21st Conference on Magnetism and Magnetic Material, Philadelphia, 1975*, AIP Conf. Proc. No. 29 (AIP, New York, 1976), p. 350]. Since that time a number of

Since that time a number of important facts have come to light, so that the present discussion constitutes a considerable revision of the interpretation given earlier.

- ⁸Similar study for the case of a non-Kondo system (*Cu Mn*) has been carried out by R. E. Walstedt and W. W. Warren, Jr., *Phys. Rev. Lett.* **31**, 365 (1973).
- ⁹M. A. Ruderman and C. Kittel, *Phys. Rev.* **96**, 99 (1954); T. Kasuya, *Prog. Theor. Phys.* **16**, 45 (1956); K. Yosida, *Phys. Rev.* **106**, 893 (1957).
- ¹⁰Small amount of curvature in the Curie-Weiss plot for 2% Mn suggested the presence of a slight systematic error in that case.
- ¹¹S. Tamaki and S. Takeuchi, *J. Phys. Soc. Jpn.* **22**, 1042 (1967).
- ¹²See, for example, the review by G. J. van den Berg, in *Progress in Low Temperature Physics*, edited by C. J. Gorter (North-Holland, Amsterdam, 1964), Vol. 4.
- ¹³J. Flouquet, *J. Phys. F* **1**, 87 (1971).
- ¹⁴A. M. Clogston, V. Jaccarino, and Y. Yafet, *Phys. Rev.* **134**, A650 (1964).
- ¹⁵Validity of this extrapolation depends on an assumed constancy of hyperfine coupling with temperature, which is generally found to be the case.
- ¹⁶J. Heighway and E. F. W. Seymour, *Phys. Kondens. Mater.* **13**, 1 (1971).
- ¹⁷A. Freeman and R. E. Watson, in *Magnetism*, edited by H. Suhl and G. Rado (Academic, New York, 1965), Vol. IIA.
- ¹⁸H. P. Myers and R. Westin, *Philos. Mag.* **8**, 1969 (1963).
- ¹⁹L. L. Hirst, *Phys. Kondens. Mater.* **11**, 255 (1970).
- ²⁰Although T_1 is very difficult to measure by the usual inversion-recovery method for values this short, such a measurement was carried out in one case, with satisfactory results, in order to check our $T_1 = T_2$ assumption.
- ²¹Concentrations shown in Fig. 2 were determined as follows. The highest concentration sample ($c = 14.7\%$) was chemically analyzed. The other two were found by scaling with the ^{209}Bi shift ΔK_{Bi} at constant temperature. Chemical analysis may tend to overestimate c because of spurious MnO present.
- ²²Phenomenological model theory developed by J. Souletie [*J. Phys. F* **5**, 329 (1975)] gives a similar variation with temperature but is at variance with the GS results for $S = \frac{1}{2}$ by a factor ~ 5 for $T \geq T_K$.
- ²³R. E. Walstedt and A. Narath, *Phys. Rev. B* **6**, 4118 (1972).
- ²⁴Y. Waseda and K. Suzuki, *Phys. Status Solidi B* **49**, 339 (1972).
- ²⁵R. E. Walstedt and L. R. Walker, *Phys. Rev. B* **11**, 3280 (1975).
- ²⁶B. Caroli, *J. Phys. F* **5**, 1399 (1975).
- ²⁷G. Malmstrom, D. J. W. Geldart, and C. Blomberg, *J. Phys. F* **6**, 233 (1976).
- ²⁸Our Bi shift data were normalized to the value given by Rossini at 860 K [F. Rossini, *Phys. Rev.* **178**, 641 (1969)].
- ²⁹J. Gardner and C. P. Flynn, *Philos. Mag.* **15**, 1233 (1967).
- ³⁰Explanation for this effect was proposed in Ref. 29 in terms of the temperature-independent susceptibility contribution which occurs for localized virtual bound states whether they are magnetized or not. That this cannot explain the observed results can be seen from the fact that it changes the neighbor shifts by the same fraction that it changes the impurity susceptibility. Thus, the intercept of a K_{Bi} vs χ_{Mn} plot would remain unchanged.
- ³¹Again, the relaxation times are very short and we assume $T_1 = T_2$ in our discussion.
- ³²Although one would correctly use the Bi-Mn radial distribution in this case, no such measurements are available and we shall make an approximate substitution of the Bi-Bi distribution in pure Bi metal.
- ³³See H. C. Torrey, *Phys. Rev.* **92**, 962 (1953).
- ³⁴Y. Waseda, F. Takahashi, and K. Suzuki, *Sci. Rep. Res. Inst. Tohoku. Univ.*, A **23**, 127 (1972).
- ³⁵N. Z. Nucker, *Z. Angew. Phys.* **27**, 33 (1969).
- ³⁶P. A. Egelstaff, *An Introduction to the Liquid State*, (Academic, New York, 1967).
- ³⁷E. F. W. Seymour, *Pure and Appl. Chem.* **40**, 41 (1974).
- ³⁸T. Chan and L. E. Ballentine, *Can. J. Phys.* **50**, 813 (1972).
- ³⁹Successful calculation of the near-field RKKY oscillations in *Cu Mn* has recently been given by J. D. Cohen and C. P. Slichter, *Phys. Rev. Lett.* **40**, 129 (1978).